Proc. Natl. Acad. Sci. USA
Vol. 78, No. 2, pp. 962–966, February 1981
Biophysics

Continuous fluorescence microphotolysis: A sensitive method for study of diffusion processes in single cells

(diffusion equation/lateral diffusion in membranes/photobleaching/sea urchin eggs)

REINER PETERS*†, AXEL BRÜNGER‡, AND KLAUS SCHULTEN‡

*Zentrum der biologischen Chemie, Universität Frankfurt, Theodor-Stern-Kai 7, 6000 Frankfurt/Main 70, Federal Republic of Germany; †Max-Planck-Institut für Biophysik, 6000 Frankfurt/Main 71, Federal Republic of Germany; and ‡Max-Planck-Institut für biophysikalische Chemie, 3400 Göttingen, Federal Republic of Germany

Communicated by Manfred Eigen, October 20, 1980

ABSTRACT **Continuous fluorescence microphotolysis is a sensitive method for the study of translational diffusion in the plasma membrane of single living cells and related systems. In this communication the conceptual basis of the method and its theoretical framework and experimental realization, as well as applications, are reported. In continuous fluorescence microphotolysis a microscopic membrane area of a single fluorescently labeled cell is irradiated by a laser beam while the fluorescence emitted from the area is monitored. The decay of the measuring signal reflects the competition of two processes: (*i*) the elimination of fluorophores by irreversible photolysis, and (*ii*) the entrance of new fluorophores into the area by diffusion. Rate constants for the two processes can be derived from the measuring data by mathematical analysis. As compared to our initial approach, fluorescence microphotolysis [Peters, R., Peters, J., Tews, K. H. & Bähr, W. (1974) *Biochim. Biophys. Acta* 367, 282–294], the main advantage of the method described here is an improvement of data quality and detection limit by orders of magnitude. From the practical point of view the main advantage is a simplification of the experimental setup. Results obtained by this method are encouraging and support the contention that continuous fluorescence microphotolysis may disclose new aspects of diffusion processes in biological systems.**

Diffusion studies on single living cells require special methods. In fluorescence microphotolysis (FM)[§] (1–6) the particular molecular species to be studied is labeled with a fluorescent marker. The diffusion measurement then proceeds in two steps. First, a small area (some μm^2) of a single cell is irradiated under a microscope by a short, intensive laser pulse (1–100 mW power), causing an instantaneous irreversible decomposition of the fluorophores. Second, the laser beam is attenuated to an extent (10–1000 nW) at which photolysis becomes negligible. The fluorescence signal excited by the attenuated laser beam indicates at which rate new fluorophores enter into the photolyzed area from the surroundings. The fluorescence recovery curve is used to derive values for the diffusion coefficient. Modifications of this general procedure have been described (2, 6, 7). Although conceptually simple and often applied, in practice FM is burdened with the requirement for advanced instrumentation (lasers, single-photon counting systems, etc.). More important, the measuring process in principle is associated with extremely low light levels, which sets a limit to the sensitivity.

Continuous fluorescence microphotolysis (CFM) is closely related to FM. As in FM, fluorescence labeling is employed. However, instead of photolysis and diffusion being separated by experimental means, both processes are allowed to occur simultaneously, their interplay being monitored and analyzed. For this purpose one irradiates a small area of a fluorescently labeled cell with a beam power of about 10 μW and monitors the decay of the fluorescence signal. The time course of the fluorescence signal originating from the irradiated area (IA) essentially depends on the rate of decomposition and on the rate at which new fluorophores enter the IA from the surroundings. By working out an adequate theory and fitting theoretical curves to experimental data the values for the diffusion coefficient and the reaction rate constant are obtained. This communication will show how the concept is put into practice.

MATERIALS AND METHODS

Reagents. Fluorescein isothiocyanate (FITC) was obtained from Sigma. Egg yolk L-α-lecithin was purchased from Calbiochem. 3,3′-Dioctadecyloxatricarbocyanine (diO) was synthesized by J. Peters according to ref. 8. Trypsin was obtained from Boehringer, Mannheim.

Lipid Vesicles. Large bilayer vesicles with diameters of up to 100 μm were formed from egg lecithin and diO (molar ratio 200:1) in distilled water as described (9).

Sea Urchin Eggs. Methods used in experiments with sea urchin eggs of the species *Paracentrotus lividus* will be described in detail elsewhere. The vitelline layer was removed from the eggs by sequential incubation with trypsin (1.5 μg/ml; 5 min; 18°C) and dithiothreitol (20 mM, 10 min, 18°C). Incorporation of diO into the egg plasma membrane was performed by incubating eggs deprived of their vitelline layer with a dye suspension (20 μg of diO per ml; 1 min; pH 8.2) in the presence of 1 vol % dimethyl sulfoxide. Labeling of membrane proteins was performed by incubation with a FITC solution (2 mg/ml; 30 min) at pH 10.0, under which conditions the dye does not penetrate into the eggs.

CFM. The apparatus used in this study is the same used for FM experiments and will be described in detail elsewhere. It consists of an argon laser (Spectra Physics, model 164-07), a fluorescence microscope with a vertical illuminator (Zeiss, Mikroskop-Photometer 03), a single-photon counting system (photomultiplier tube RCA, model 8850; Ortec components 456, 9302, 9315, 9320, 779), and a small computer (Heath HW 89). The laser was operated at 4765 Å and 100 mW. The beam power could be attenuated by a series of neutral density filters. The laser beam was directed into the entrance of the vertical illuminator. In front of the entrance, at an image plane of the optical system of the microscope, a diaphragm with a diameter of 400 μm was inserted into the laser beam. The central part of the laser beam passing the diaphragm was imaged into the object by

The publication costs of this article were defrayed in part by page charge payment. This article must therefore be hereby marked "*advertisement*" in accordance with 18 U. S. C. §1734 solely to indicate this fact.

Abbreviations: CFM, continuous fluorescence microphotolysis; FM, fluorescence microphotolysis; FITC, fluorescein isothiocyanate; diO, 3,3′-dioctadecyloxatricarbocyanine; IA, irradiated area.

§ Synonyms for FM are FPR, fluorescence photobleaching recovery, and FRAP, fluorescence recovery after photobleaching.

the objective (Planapo ×100). This procedure yielded a circular IA with a diameter of 4.0 μm and a virtually uniform intensity distribution. Fluorescence emitted by the object was directed into the microphotometric attachment, passed through a square field diaphragm, and reached the cathode of the photomultiplier tube. In the experiment the laser beam initially was blocked by an electromagnetic shutter. The measurement was initiated by opening the shutter and, at the same time, triggering the photon counting system. The counting interval was adjusted to the kinetics of the fluorescence decay and ranged from 30 ms for diffusion coefficients $D \geq 1\ \mu m^2\ s^{-1}$ to 2 s for $D \leq 0.01\ \mu m^2\ s^{-1}$. All measurements were performed at 20°C.

RESULTS AND DISCUSSION

Concept and Theory. We illustrate the CFM method by its application to the diffusion of the fluorescent lipid analogue diO in lipid vesicles. As a first approximation we assume the following simplified reaction scheme. Irradiation of a small circular area of radius a leads to excitation and irreversible photolysis of diO:

$$\text{diO} \underset{\text{fluorescence}}{\overset{h\nu}{\rightleftharpoons}} \text{diO}^* \xrightarrow{\text{photolysis}} \text{P}$$

The fluorescence signal shown in Fig. 1 serves as a measure of the concentration of nonphotolyzed diO in the IA. If the fluorophores were immobile, irradiation and photolysis under the conditions of a first-order reaction and a homogeneous light level in the IA would lead to a simple exponential decay of the fluorophore concentration and, hence, of the fluorescence signal. Any mobility of the dye, for example due to diffusion or a laminar flow, would replenish the fluorophores in the IA and, thereby, shift the fluorescence signal above an exponential decay curve. Such behavior is, in fact, observed in Fig. 1. The signal exhibits an initial fast decay followed by a slower decay, a behavior clearly indicative of lateral motion of the dye in the membrane. The close agreement in Fig. 1 between the observed signal and a theoretical description based on a diffusion model (see below) demonstrates that the motion of the dye is due to diffusion in the membrane plane. The fit between observation and theory actually is the basis of the CFM method and yields the diffusion coefficient D.

The behavior of the fluorescence signal in Fig. 1 reflects the competition between a photoreaction and a diffusion process.

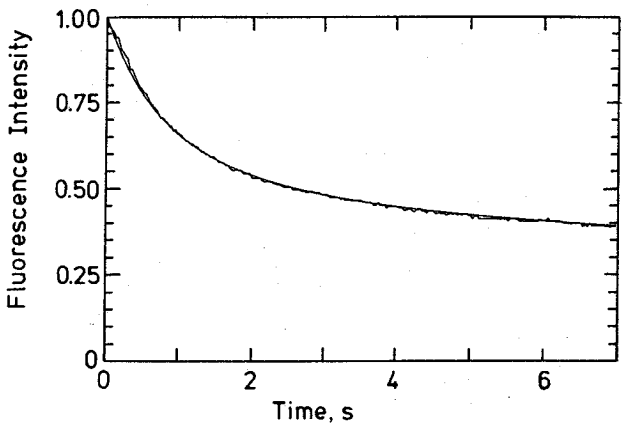

FIG. 1. Comparison of observed and fitted time-dependent fluorescence intensity during the CFM of the fluorescent lipid analogue diO in the membranes of large artificial vesicles made from egg lecithin; temperature = 20°C; the irradiated area had a radius $a = 2\ \mu m$; the fitted curve corresponds to $k_0 = 0.73\ s^{-1}$ and $D = 1.4\ \mu m^2\ s^{-1}$, the diffusion space being limited to an area $r \leq R = 20\ \mu m$.

Assuming first-order kinetics with a rate constant k_0, the photoreaction is characterized by a time scale $\tau_{ph} = k_0^{-1}$. The relevant time scale for the diffusion process is given by the mean time $\tau_d = a^2/D$ for the dye to diffusively cross the IA. The accuracy of the CFM method is best when $\tau_{ph} \approx \tau_d$. In the case that $\tau_{ph} \ll \tau_d$, the fluorescence signal would closely follow an exponential decay signalling solely the photoprocess. In the case that $\tau_{ph} \gg \tau_d$, diffusion would replenish the dye as soon as photolysis occurred and the fluorescence signal would exhibit only a minor initial decrease. Both limiting cases would be very difficult to analyze in terms of a diffusion coefficient. Fortunately, by a proper choice of the size of the IA and of the light intensity one is free to choose τ_{ph} close to τ_d. In our experimental setup both the light intensity and the IA can be varied by a factor larger than 10^2, which allows us to explore D values through more than 6 orders of magnitude.

The CFM measurement in Fig. 1 corresponds to a τ_{ph}/τ_d ratio of about 0.5. In this situation of optimal accuracy the fluorescence signal is characterized by two time regimes. In the first regime the decay is fast, in the second it is slower. The fast decay reflects the events occuring in the IA and its immediate surroundings. Fluorophores initially located in the IA are photolyzed and, concomitantly, fresh fluorophores enter the IA from the immediate surroundings. The decay depends only on k_0, D, and a, and not on the overall geometry of the system (e.g., shape and size of the lipid vesicle). The fast decay ends when a "quasi-stationary" state is reached in which the rates of photolysis and diffusive influx are nearly equal. The slow phase of the decay curve, on the other hand, reflects the depletion of fluorophores from distant parts of the membrane. This decay depends on k_0, D, and a and on the size of the whole diffusion space around the IA.

Early Time Regime of the Fluorescence Decay. Because we are interested primarily in obtaining diffusion coefficients and not the system size, we have chosen to analyze the initial part of the fluorescence decay curve. The theoretical description of the reaction–diffusion process of CFM requires a numerical solution that can be found with a desk-top computer. In the early time regime of the fluorescence decay curve one can assume radial symmetry for the IA and its surroundings. The equation that governs the time development of the concentration $p(r,t)$ of nonphotolyzed fluorophores—i.e., of the number of fluorophores found at radius r from the center of the IA at time t—is

$$\frac{\partial p(r,t)}{\partial t} = l(r)\,p(r,t) - k(r)\,p(r,t), \qquad [1]$$

in which the differential operator

$$l(r) = D\left(\frac{\partial^2}{\partial r^2} + \frac{1}{r}\frac{\partial}{\partial r}\right) \qquad [2]$$

describes the planar diffusion, and the scalar operator

$$-k(r) = \begin{cases} -k_0 \text{ for } r \leq a \\ 0 \text{ for } r > a \end{cases} \qquad [3]$$

describes the depletion by the photoreaction. This functional form of $k(r)$ assumes a homogeneous light intensity in the IA as realized in our experimental setup. However, $k(r)$ may be chosen so as to account for any intensity profile and also for any time dependence. A nonlinear reaction behavior could also be incorporated in Eq. 1. The numerical algorithm best suited to obtain $p(r,t)$ is the Crank–Nicholson scheme (10).¶

¶ Details will be published elsewhere; an outline of the theory and a FORTRAN or BASIC program for the calculation of the CFM fluorescence signals will be provided upon request.

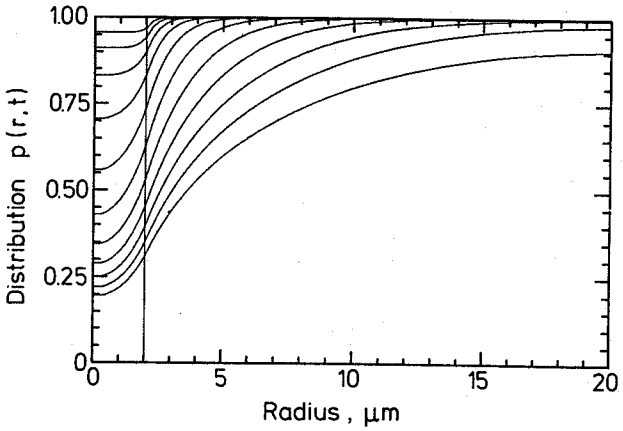

FIG. 2. Predicted time development of the dye distribution $p(r,t)$ corresponding to Fig. 1 ($a = 2$ μm, $R = 20$ μm, $k_0 = 0.73$ s^{-1}, and $D = 1.4$ μm^2 s^{-1}); the distributions are taken at times 0.0625, 0.125, 0.25, 0.5, 1, 2, 4, 8, 16, 32, and 64 s; the area irradiated is indicated by the vertical line.

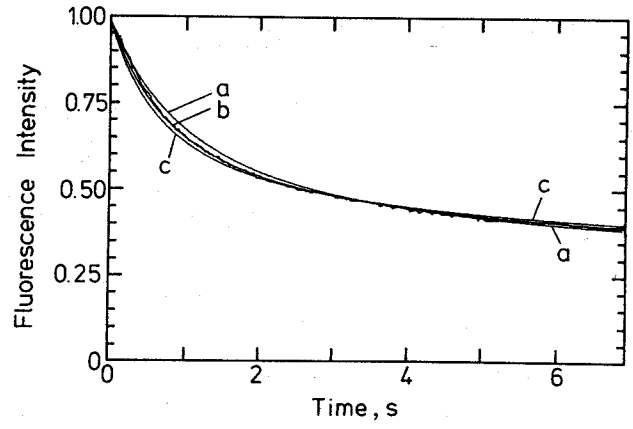

FIG. 3. Comparison of the observed and calculated time-dependent fluorescence intensities to demonstrate the accuracy of the diffusion coefficients as determined by CFM; the observation and the best fit (curve b) are taken from Fig. 1, curve c and curve a correspond to k_0, D values of 0.85 s^{-1}, 1.8 μm^2 s^{-1} and 0.60 s^{-1}, 0.95 μm^2 s^{-1}, respectively.

The concentration profiles $p(r,t)$ predicted by Eq. 1 for the CFM measurement in Fig. 1 are presented in Fig. 2 for various times. Initially ($t = 0$) the dye concentration is constant throughout. The photoreaction then begins to deplete the IA of fluorophores as shown by the profiles at later times. Diffusion tends to replenish the fluorophores in the IA, whereby the fluorophore concentration in the surroundings slowly decreases. Fig. 2 demonstrates that up to 7 s, which is the time period of Fig. 1, the decrease of the concentration profile extends only to a radius of 10 μm. This illustrates clearly that the early phase of the fluorescence decay curve involves only diffusion from the immediate surroundings of the IA.

Late Time Regime of the Fluorescence Decay. The slow decay of the fluorescence signal reflects the gradual depletion of the dyes in the whole membrane due to the diffusion of dyes towards the IA and the subsequent photoreaction. Because, in general, the long-distance diffusion takes more time than the photoreaction, the corresponding decay is mainly sensitive to the diffusion process and the geometry of the diffusion space. If one approximates the slow decay by a single exponential, one can derive the following simple expression for the decay constant τ_s[¶] ($x = \tau_D/4\tau_{ph}$, $y = a/R$):

$$\tau_s = \left(\frac{R^2}{D}\right)\left(\frac{y^2-3}{8} - \frac{\ln y}{2(1-y^2)} + \frac{1-y^2}{4f(x)}\right), \quad [4]$$

$$f(x) = \frac{x\left(1 + \frac{x}{1!2!} + \frac{x^2}{2!3!} + \cdots\right)}{1 + \frac{x}{1!1!} + \frac{x^2}{2!2!} + \cdots} \quad [5]$$

The derivation is based on the assumption of a quasistationary distribution $I_0(\sqrt{k_0/D}\, r)$ in the IA, $I_0(x)$ representing the modified zero-order Bessel function. The logarithmic derivative of this distribution at $r = a$ according to ref. 11 yields expressions 4 and 5. τ_s may be matched to the observed slow decay to yield information on the size R of the diffusion domain. The single exponential approximation holds for moderate values of R/a. For example, for the situation corresponding to Fig. 1, $\tau_s = 403$ s compares well with the late time regime relaxation time, numerically determined to be 386 s.

Accuracy of the Method. Because in CFM the photoreaction is coupled to the diffusion process, any uncertainty connected with the former leads to increased error in the analysis. Uncertainties regarding the photoprocess relate to any deviation from first-order kinetic behavior (Eq. 1) and also originate from the need for a fit of the reaction rate constant k_0. In Fig. 3 decay curves corresponding to the fit in Fig. 1 are compared to decay curves resulting for D values fixed at ±30% of the optimal value and k_0 values chosen to obtain close agreement with the measured fluorescence signal. The two resulting decay curves lie just outside of the scatter of the signal; i.e., the D values determined by a fitting procedure should be accurate within ±30%. Naturally, any further increase of the variation space—e.g., to account for the possible existence of several dye species with different D and k_0—would add to the uncertainties of these constants. However, if independent knowledge of the photokinetics is available the accuracy of D can be increased. In closing, we point out that the best D value of 1.4 μm^2 s^{-1} obtained by CFM agrees with the value of 1.6 μm^2 s^{-1} that we have obtained by FM measurements on the same vesicle preparations. D values obtained by various other methods on comparable vesicle or multibilayer preparations are 1.2 μm^2 s^{-1} (9), 3 μm^2 s^{-1} (12), 1.5 μm^2 s^{-1} (13), and, in marked deviation, 16 μm^2 s^{-1} (14).

Sensitivity. CFM permits one to measure diffusion in systems containing only a small number of fluorescent molecules. The lower limit of CFM sensitivity has been estimated by mea-

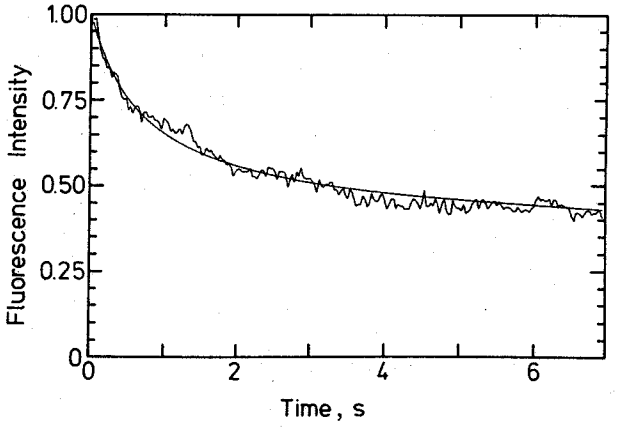

FIG. 4. Time-dependent fluorescence intensity during the CFM ($a = 2$ μm) of a 35 nM FITC solution in a glycerol/water mixture (90:10, wt/wt); the fitted curve corresponds to $k_0 = 0.91$ s^{-1} and $D = 2.3$ μm^2 s^{-1} ($R = 20$ μm).

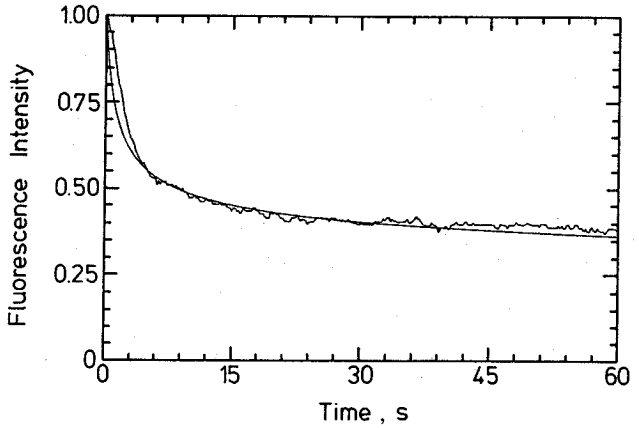

FIG. 5. Time-dependent fluorescence intensities during the (*repeated*, see text) CFM ($a = 2\ \mu m$) of the fluorescent lipid analogue diO in the plasma membrane of sea urchin eggs; the calculated curve corresponds to a diffusion coefficient of 1.5 $\mu m^2\ s^{-1}$ ($k_0 = 0.52\ s^{-1}$, $R = 20\ \mu m$).

surements on solutions with known numbers of fluorophores. An example is given in Fig. 4, in which FITC has been dissolved in a mixture of glycerol and 10 mM sodium carbonate buffer, pH 10 (90:10, wt/wt) at a concentration of 35 nM. The FITC concentration has been checked by photometric measurements, using an extinction coefficient of $8.08 \times 10^4\ M^{-1}\ cm^{-1}$ at 484 nm (15). Samples (1.0 μl) were allowed to spread uniformly between clean slides and 24 × 24 mm coverslips yielding layers of 1.75 μm average thickness. Hence, the average volume of test solution in the IA (radius 2 μm) was 22×10^{-15} liter and the average initial number of FITC molecules was approximately 500. Background fluorescence as determined on samples of pure solvent has been subtracted from the data for the FITC-containing specimen.

Fig. 4 shows that a reasonable measuring signal is obtained for very small fluorophore numbers. The measured value for the diffusion coefficient, $D = 2.3\ \mu m^2\ s^{-1}$, is close to expectation. To our knowledge, the diffusion of FITC in glycerol/water mixtures has not been studied before. For an estimate we assume that the diffusion coefficient of FITC in pure water is close to that of sucrose, namely 522.6 $\mu m^2\ s^{-1}$ (16). The relative viscosity η/η_0 of glycerol/water at 90:10 (wt/wt) is about 230 (16) and, according to the Stokes–Einstein relationship, one expects then a diffusion coefficient of 2.25 $\mu m^2\ s^{-1}$ for FITC in this glycerol/water solution.

Application to a Biological Membrane. As an example for the application of CFM to the study of diffusion processes in single living cells, we have measured the mobility of diO and of FITC-labeled proteins in the plasma membrane of sea urchin eggs. In biological membranes a fraction of the labeled molecules is frequently immobile. In order to determine the magnitude of this fraction, CFM measurements routinely were performed two or more times at the same location of individual eggs. Intervals between measurements were large enough so as to allow for redistribution of the labeled molecules to equilibrium. The outcome (not shown) of this procedure consistently was that the initial fluorescence intensity in the first measurements, J_0^I, was higher than the initial intensities in the second and in the following measurements, $J_0^{II}, J_0^{III}, \cdots$. Clearly, a certain fraction of the fluorophores that was photolyzed in the first measurement could not be exchanged for fresh molecules. The immobile fraction was determined as $(J_0^I - J_0^{II})/J_0^I$ and amounted in the case of the sea urchin egg to 10% for both diO and FITC-labeled proteins. D values were derived always from the second or a following measurement of diO diffusion.

A measurement of diO diffusion is shown in Fig. 5. It is obvious that in this case a close fit between experiment and theory could not be obtained. Because in other cases of diO diffusion (see Fig. 1) a good fit had been obtained, the discrepancy apparently is due to the organization of the sea urchin membrane. It comes to mind that the egg surface is not smooth but rather irregular (17). However, CFM data on protein diffusion in the same membrane can be fitted very well. A CFM experiment on FITC-labeled eggs is given in Fig. 6. The data reveal an undulation, which might be related to pulsations of the whole egg or rhythmic processes in the egg cortex. The CFM measurement (Fig. 6*a*) was followed by a series of measurements (Fig. 6*b*) demonstrating the redistribution of the FITC-labeled proteins in the dark.

CFM Versus FM. If CFM and FM experiments are performed with the same specimen the signal-to-noise ratio of the measuring signal is much better in CFM than in FM. Basically this is due to the fact that, during fluorescence measurement, a photolytic decomposition of the fluorophores has to be avoided in FM, whereas such decomposition is essential for CFM. Hence, excitation levels have to be low in FM, but are some orders of magnitude larger in CFM.

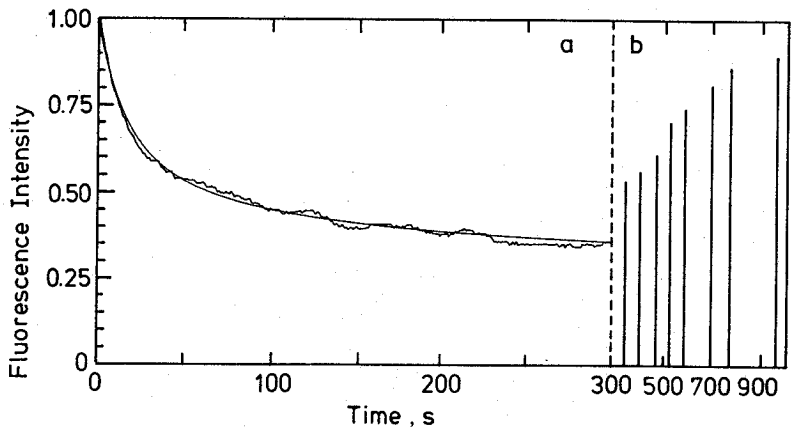

FIG. 6. (*a*) Time-dependent fluorescence intensity during the (*repeated*) CFM ($a = 2\ \mu m$) of FITC-labeled proteins in the plasma membrane of sea urchin eggs; the calculated curve corresponds to a diffusion coefficient of 0.08 $\mu m^2\ s^{-1}$ ($k_0 = 0.037\ s^{-1}$, $R = 20\ \mu m$); (*b*) Observation of the recovery of the fluorescence intensity after 300 s of CFM due to back diffusion of the dye into the IA; measurements were taken by a series of short probe light flashes.

Improvement of data quality in CFM has two major consequences: (*i*) details of diffusion processes not detected by other methods may be revealed (Figs. 5 and 6) and (*ii*) measurements may be extended to lower fluorophore concentrations (Fig. 4). A few hundred fluorophores per reaction area are sufficient to obtain a measuring signal of reasonable quality. Taking into account that the immediate neighborhood of the IA is depleted of fluorophores in the course of a measurement, we estimate that a few thousand fluorophores are sufficient for determinations of *D* values. Because molecular species of great functional significance such as hormone receptors (18) frequently occur as only a few thousand copies per cell, this aspect may be of particular relevance.

CFM requires less instrumentation than FM. Devices for creating laser flashes as well as mechanisms for the protection of the photomultiplier from the flashes can be dispensed with. Advanced low-level light detection systems frequently may be unnecessary and lasers may be replaced by conventional light sources—e.g., high-pressure mercury lamps.

Thermal and photochemical effects of laser radiation are a potential source of artifacts in both FM and CFM. All available evidence—as summarized and discussed in ref. 19—shows that such effects as localized heating, oxidation, and crosslinking do not play a significant role in FM measurements of living cells. Comparing CFM with FM in this respect, the essential features are that the total radiation dose per measurement is about equal in both methods, whereas the radiation intensity is lower in CFM than in FM. The study of Sheetz and Koppel (20) suggests that, for radiation doses being equal, lower intensities yield higher degrees of crosslinking. The risk of photochemical damage would then be higher in CFM than in FM. However, in CFM the fluorophore concentration can be much lower than in FM and, accordingly, the risk of crosslinking could be reduced in CFM. Furthermore, the study of Sheetz and Koppel (20) concerns isolated membranes. In living cells the situation is quite different because substances are present (e.g., glutathione) that can prevent crosslinking when added to isolated membranes (20).

Outlook. Involving two simultaneous processes—diffusion and photolysis—CFM is more complex than FM. In order to interpret the experimental data we have used the most simple theoretical model combining diffusion and a first-order reaction. Application of this model has led to satisfactory results. However, in order to exploit the full power of the method it is desirable to obtain detailed knowledge on the kinetics of the photochemical processes—e.g., by observing the fluorescence signal in the center of a very large IA. This may be seen as a principal objective of further studies.

R.P. thanks Dr. Jutta Peters for synthesizing diO. A.B. has been supported by the Studienstiftung des Deutschen Volkes. K.S. thanks the Kultusministerium des Landes Niederachsen for a Jerusalem–Göttingen exchange grant. R.P. gratefully acknowledges support by the Deutsche Forschungsgemeinschaft.

1. Peters, R., Peters, J. & Tews, K. H. (1974) *Pflügers Arch.* **347**, R36 (abstr.).
2. Peters, R., Peters, J., Tews, K. H. & Bähr, W. (1974) *Biochim. Biophys. Acta* **367**, 282–294.
3. Edidin, M., Zagyanski, Y. & Lardner, T. J. (1976) *Science* **191**, 466–468.
4. Jacobson, K., Wu, E. & Poste, G. (1976) *Biochim. Biophys. Acta* **433**, 215–222.
5. Axelrod, D., Koppel, D. E., Schlessinger, J., Elson, E. & Webb, W. W. (1976) *Biophys. J.* **16**, 1055–1069.
6. Smith, B. A. & McConnell, H. M. (1978) *Proc. Natl. Acad. Sci. USA* **75**, 2759–2763.
7. Koppel, D. E. (1979) *Biophys. J.* **28**, 281–292.
8. Sondermann, J. (1971) *Justus Liebigs Ann. Chem.* **749**, 183–197.
9. Fahey, P. F. & Webb, W. W. (1978) *Biochemistry* **17**, 3046–3053.
10. Richtmeyer, R. D. & Morton, K. W. (1967) *Difference Methods for Initial Value Problems* (Wiley, New York), pp. 189, 198.
11. Szabo, A., Schulten, K. & Schulten, Z. (1980) *J. Chem. Phys.* **72**, 4350–4357.
12. Träuble, H. & Sackmann, E. (1972) *J. Am. Chem. Soc.* **94**, 4499–4511.
13. Cullis, P. R. (1976) *FEBS Lett.* **70**, 223–228.
14. Wu, E.-S., Jacobson, K. & Papahadjopoulos, D. (1977) *Biochemistry* **16**, 3936–3941.
15. de Petris, S. (1978) in *Methods in Membrane Biology*, ed. Korn, E. D. (Plenum, New York), Vol. 9, p. 155.
16. Weast, R. C. & Astle, M. J., eds. (1979) *CRC Handbook of Chemistry and Physics* (CRC Press, Boca Raton, FL), 60th Ed., pp. F-62, D-239.
17. Tegner, M. J. & Epel, D. (1973) *Science* **179**, 685–688.
18. Cuatrecasas, P. (1974) *Annu. Rev. Biochem.* **43**, 169–214.
19. Wolf, D. E., Edidin, M. & Dragsten, P. R. (1980) *Proc. Natl. Acad. Sci. USA* **77**, 2043–2045.
20. Sheetz, P. M. & Koppel, D. E. (1979) *Proc. Natl. Acad. Sci. USA* **76**, 3314–3317.